PAPER

Ultrafast reduction of exchange splitting in ferromagnetic nickel

IOP Publishing Journal of Physics: Condensed Matter
J. Phys.: Condens. Matter **28** (2016) 236004 (8pp) doi:10.1088/0953-8984/28/23/236004

Ultrafast reduction of exchange splitting in ferromagnetic nickel

G P Zhang[1], Y H Bai[2] and Thomas F George[3]

[1] Department of Physics, Indiana State University, Terre Haute, IN 47809, USA
[2] Office of Information Technology, Indiana State University, Terre Haute, IN 47809, USA
[3] Departments of Chemistry & Biochemistrony and Physics & Astronomy, Office of the Chancellor and Center for Nanoscience, University of Missouri-St. Louis, St. Louis, MO 63121, USA

E-mail: gpzhang@indstate.edu

Received 8 March 2016, revised 16 April 2016
Accepted for publication 21 April 2016
Published 10 May 2016

Abstract

A decade ago Rhie *et al* (2003 *Phys. Rev. Lett.* **90** 247201) reported that when ferromagnetic nickel is subject to an intense ultrashort laser pulse, its exchange splitting is reduced quickly. But to simulate such reduction remains a big challenge. The popular rigid band approximation (RBA), where both the band structure and the exchange splitting are held fixed before and after laser excitation, is unsuitable for this purpose, while the time-dependent density functional theory could be time-consuming. To overcome these difficulties, we propose a time-dependent Liouville and density functional theory (TDLDFT) that integrates the time-dependent Liouville equation into the density functional theory. As a result, the excited charge density is reiterated back into the Kohn–Sham equation, and the band structure is allowed to change dynamically. Even with the ground-state density functional, a larger demagnetization than RBA is found; after we expand Ortenzi's spin scaling method into an excited-state (laser) density functional, we find that the exchange splitting is indeed strongly reduced, as seen in the experiment. Both the majority and minority bands are shifted toward the Fermi level, but the majority shifts a lot more. The ultrafast reduction in exchange splitting occurs concomitantly with demagnetization. While our current theory is still unable to yield the same percentage loss in the spin moment as observed in the experiment, it predicts a correct trend that agrees with the experiments. With a better functional, we believe that our results can be further improved.

Keywords: exchange splitting, laser-induced, ultrafast, ferromagnetic, density functional theory, Liouville equation, nickel

(Some figures may appear in colour only in the online journal)

1. Introduction

Laser-induced ultrafast demagnetization [1–3] presents a new opportunity for magnetic storage technology, as it significantly shortens the read/write time [4], a necessity for large data storage devices. This has attracted extensive investigations both theoretically [5–22] and experimentally [23–31]. The method of choice to investigate such a fast demagnetization is the time-resolved magneto-optical Kerr effect (TRMOKE). Despite earlier debates [21, 32] on the suitability of TRMOKE for femtomagnetism [2], it is now generally agreed that by carefully removing the nonmagnetic contribution from the Kerr ellipticity and rotation signal, one can access the spin moment change in the time domain. Such a connection has been established by comparing and contrasting the optical and magnetic response functions using the first-principles method [33, 34]. Recently, an analytic relation has been found between the spin angular momentum and the off-diagonal susceptibility [35]. Another technique which complements TRMOKE is the time- and spin-resolved photoemission (TSRPE). It is capable of resolving the spin momentum change in the crystal momentum space [36]. In TSRPE, a laser pulse first excites electrons from the spin-polarized valence band to the conduction band, and a second pulse ionizes the

electrons to the vacuum. Since the energy of the emitted spin-polarized electron reflects its original valence band energy, the exchange energy splitting can be monitored. However, whether the exchange splitting is collapsed has been controversial. The first TSRPE was reported a long time ago [37], but the result has not been reproduced. More recent experimental studies are extended to Gd. Carley *et al* [38] investigated the exchange-split Σ valence bands of gadolinium and found that the majority and minority bands both move closer to the Fermi surface, but differ on the time scale. In a ferromagnetic nickel thin film, Rhie *et al* [39] demonstrated the collapse of the magnetic exchange splitting. Pickel *et al* [40] used photoemission to identify the spin–orbit hybridization points in fcc Co. Weber *et al* [41] tried to compare TRMOKE with TSRPE, but their results were not conclusive since different experimental conditions were used for TRMOKE and TSRPE. In Fe, Carpene *et al* [42] showed recently that the modification of the electronic band structure upon laser excitation is small, but argued that in nickel the collapse of the exchange splitting might be justified.

Theoretically, several different approaches are available. One is based on the rigid band approximation (RBA) [43–46], which has been used in semiconductors [47, 48] as well as ferromagnets [5, 10, 14]. Under RBA, the band structure is not allowed to change before and after laser excitation, and thus it fixes the exchange splitting. For this reason, RBA is unsuitable for the exchange splitting. It has been argued that the rigid band structure calculations will never be in quantitative agreement with experiments, irrespective of the investigated microscopic scattering mechanism [20]. In a simplified model calculation, Mueller *et al* [49] proposed a scheme that allows the charge density to dynamically affect the exchange splitting change, which they call the feed-back effect. More recently, the time-dependent density functional theory (TDDFT) was employed to investigate the demagnetization [19], but it is very time-consuming to carry out such a calculation. This motivated Wang *et al* to develop a two-step time propagation [50].

In this paper, we propose an alternative scheme to TDDFT, which is less time-consuming. We merge the standard density functional theory (DFT) with the time-dependent Liouville equation, so the excited-state density is reiterated back into the Kohn–Sham (KS) equation, thus going beyond the rigid band approximation. The self-consistent calculation converges the KS orbitals on the excited-state potential surface, different from the ground-state calculation. We call this scheme the time-dependent Liouville density functional theory, or TDLDFT. We find that even with the ground-state functional, the demagnetization is an order of magnitude larger than RBA. Since most of the existing exchange correlation functionals are geared toward the ground-state properties, to properly describe the excited-state property, we implement a functional based on the Ortenzi spin scaling function, where the spin polarization acts upon the system self-consistently. We find that both the majority and minority bands are shifted toward the Fermi surface, but the amount of shift is different. The majority band moves upward by 0.26 eV, while the minority one moves downward by only 0.03 eV. As a result, the exchange splitting is reduced. Interestingly, we find that the exchange splitting change correlates well with the spin moment change in ferromagnetic nickel. We have tested three functionals, with the largest spin moment reduction reaching 10%. Although this is still below the experimental value, the trend seems promising. With a better functional, we expect that our results can be systematically improved upon.

The rest of the paper is arranged as follows. In section 2, we present the theoretical formalism. Section 3 is devoted to the results and discussions on (i) the comparison between the rigid-band approximation and the TDLDFT calculation, (ii) the development of the excited-state (laser) functionals, and (iii) the collapse of the exchange splitting. The paper is concluded in section 4.

2. Time-dependent Liouville density functional theory (TDLDFT)

Our new idea comes from an important observation. After a laser pulse impinges on a 3*d* magnet, a few electrons are excited out of the Fermi sea, with 3*d* holes left behind. It is important to realize that losing a few electrons around the Fermi level will significantly weaken the exchange correlation [49, 51–53], creating a new potential for the entire system and setting off an avalanche of spin change. In the many-body picture [54], the electron dynamics takes place on an excited-state potential surface that can be very different from the ground-state one. In the density functional theory, the many-body correlation effect is captured through the exchange-correlation functional, but now one has to solve the Kohn–Sham equation self-consistently, so *the new potential must act upon itself*. We tested this idea of a static version of this method in a prior study [51], where we saw a big effect on the spin moment.

In our new algorithm, we first solve the Kohn–Sham equation for the ground state,

$$\left[-\frac{\hbar^2\nabla^2}{2m_e}+v^{\sigma}_{\rm eff}(\mathbf{r})\right]\psi^{\sigma}_{i\mathbf{k}}(\mathbf{r})=E^{\sigma}_{i\mathbf{k}}\psi^{\sigma}_{i\mathbf{k}}(\mathbf{r}). \tag{1}$$

Here the first term on the left-hand side is the kinetic energy, $\psi^{\sigma}_{i\mathbf{k}}(\mathbf{r})$ and $E^{\sigma}_{i\mathbf{k}}$ are respectively the eigenstate and eigenenergy of band i and $\mathbf{k}$ point with spin σ, and $v^{\sigma}_{\rm eff}$ is determined by

$$v^{\sigma}_{\rm eff}(\mathbf{r})=v^{\sigma}(\mathbf{r})+\int\frac{\rho^{\sigma}(\mathbf{r}')}{|\mathbf{r}-\mathbf{r}'|}{\rm d}\mathbf{r}'+v^{\sigma}_{\rm xc}(\mathbf{r}), \tag{2}$$

where $v^{\sigma}_{\rm xc}(\mathbf{r})$ is the exchange-correlation potential, $v^{\sigma}_{\rm xc}(\mathbf{r})=\delta E_{\rm xc}[\rho^{\sigma}]/\delta\rho(\mathbf{r})$. We use the generalized gradient approximation for the exchange-correlation energy functional. The spin–orbit coupling is included through the second-variational method [55], so the following wavefunctions and eigenvalues have no spin index.

The laser excitation is computed by the time-dependent Liouville equation [33, 34],

$${\rm i}\hbar\frac{\partial\rho_{\mathbf{k},ij}}{\partial t}=[H_0+H_{\rm I},\rho_{\mathbf{k},ij}], \tag{3}$$

where $\rho_{\mathbf{k},ij}$ is the density matrix element between band states i and j at the $\mathbf{k}$ point, H_{I} is the interaction between the laser and the system (see below for details), and H_0 is the unperturbed Hamiltonian, $H_0 = \sum_{i\mathbf{k}} E_{i\mathbf{k}} |\psi_{i\mathbf{k}}\rangle\langle\psi_{i\mathbf{k}}|$. Different from the rigid-band approximation (RBA), we only integrate a small time step, Δt, typically one-eighth of the laser period, but within Δt, we solve equation (3) accurately with a high tolerance of 5×10^{-14}. This method is identical to that of Wang *et al* [50] who separate a single time step into two time steps by expanding the real time wavefunction in terms of the adiabatic eigenstate $\psi_{i\mathbf{k}}(\mathbf{r}, t)$ of the Hamiltonian at a specific time step, while $\psi_{i\mathbf{k}}(\mathbf{r}, t)$ is only approximately propagated. Here we do not extrapolate between two time steps since the spin excitation is much slower.

In the time-dependent density functional theory (TDDFT) [56][4], the time-dependent Kohn–Sham equation is solved in real time with a very tiny time step since the time step is directly linked to the inverse of the total energy, so TDDFT is often limited to an extremely short time scale. The new density is computed by

$$\rho(\mathbf{r}, t) = \sum_{i\mathbf{k}} n_{i\mathbf{k}} \psi^*_{i\mathbf{k}}(\mathbf{r}, t)\, \psi_{i\mathbf{k}}(\mathbf{r}, t), \tag{4}$$

where $n_{i\mathbf{k}}$ is the occupation number and is fixed in time from the beginning. In TDLDFT,

$$\rho(\mathbf{r}, t) = \sum_{i\mathbf{k}} \rho_{\mathbf{k};ii}(t)\, \psi^*_{i\mathbf{k}}(\mathbf{r}, t)\, \psi_{i\mathbf{k}}(\mathbf{r}, t), \tag{5}$$

where $\rho_{\mathbf{k};ii}$ is computed from the Liouville equation (equation (3)). In TDLDFT $\psi_{i\mathbf{k}}(\mathbf{r}, t)$ is the adiabatic eigenstate at time t and is not solved from the time-dependent Kohn–Sham equation, thus saving lots of time, and is useful for long-time dynamics that is actually observed experimentally, in contrast to TDDFT. The time step size is determined by equation (3). As one may realize from equation (3), the Liouville equation gives the density matrix, not the density itself. But since the premise of the density functional theory is that the exchange-correlation potential is a functional of the density, not the density matrix, when we assemble the density $\rho(\mathbf{r}, t)$, the off-diagonal density matrix elements of $\rho_{\mathbf{k};ij}$ are discarded. This points out a possible extension of our current formalism in the future.

To catch the many-body excitation, we iterate the resultant density $\rho(\mathbf{r}, t)$ back into the Kohn–Sham equation (1) and solve it self-consistently under this excited density and thus the time-dependent potential $v_{\mathrm{eff}}(\mathbf{r}, t)$. Such a self-consistent calculation is crucial since it essentially allows the excited density to affect upon the system itself and thus catches majority of the missing electron correlation and many-body effects in RBA. Figure 1(b) compares our TDLDFT algorithm (see the flowchart with red arrows) with the RBA one (see the flowchart with black arrows). The TDLDFT employs an idea similar to a prior study by Mueller *et al* [49], who only implemented it for a model system, but there are several major differences. Our method is implemented at the first-principles level. We do not shift the bands manually; instead we include the spin–orbit coupling to allow the spin change. In comparison with TDDFT, the Liouville formalism-based TDLDFT has another advantage. It naturally respects the Pauli exclusion principle, which is extremely important for the system with many electrons at a single $\mathbf{k}$ point. Once excited by laser pulses, the occupation can be dynamically changed, without fixing the occupation for the entire dynamics, which is closer to real dynamics.

[4] Extensive references can be found in [56].

3. Results and discussions

To demonstrate the power of TDLDFT, we take fcc Ni as an example. Different from prior studies [19], our laser parameters are very close to the experimental ones [1]. The interaction between the laser field and the system is [57]

$$H_{\mathrm{I}} = \frac{e}{m}\, \mathbf{p} \cdot \mathbf{A}(t), \tag{6}$$

where $-e$ is the electron charge, m is the electron mass, $\mathbf{p}$ is the momentum operator, and the vector potential $\mathbf{A}(t)$ is along the z axis with a Gaussian shape $|\mathbf{A}(t)| = A_0 \exp(-t^2/\tau^2)\cos(\omega t)$, with $A_0 = 0.03$ V fs Å^{-1}. The duration is $\tau = 60$ fs and the photon energy $\hbar\omega$ is 2 eV, corresponding to the experimental wavelength of 620 nm [1]. We note that the TDDFT study [19] used the three photon energies, i.e. 1.35, 2.73 and 5.42 eV, which do not match any experimental one. Since TDDFT is very time-consuming, an extremely short pulse was used. For the same reason, the number of $\mathbf{k}$ points was only $(8 \times 8 \times 8)$, too few to converge the results [58]. This makes the TDDFT results difficult to compare with the experimental ones. In our study, we use a $\mathbf{k}$ mesh of $(30 \times 30 \times 30)$, and we test its convergence using a larger number of $\mathbf{k}$ points. The transition matrix element for the momentum operator is directly computed using WIEN2k's optic code [59].

3.1. Comparison between the rigid-band approximation and TDLDFT calculation

To have a quantitative understanding of the spin moment reduction, figure 2(a) compares the RBA and TDLDFT spin moments as a function of time [33]. Under RBA (long dashed line), the spin moment reduces quickly from 0.637 μ_{B} to the minimum of 0.627 μ_{B} around 0 fs, but soon recovers to 0.634 μ_{B}, or 0.47%, consistent with our prior study [10] and also others [20]. In the following, we define the time at the spin moment minimum as the demagnetization time τ_{M}. Such a sharp reduction and quick recovery is the hallmark of the system overheating, where the electrons are temporally held by the laser field in the excited states (electrons are field-dressed), and they can not pass the excessive energy to other unexcited electrons beyond the parent $\mathbf{k}$ point within a single-particle picture [36]. Once the laser is gone, only a few electrons are left in the excited states and majority of the excited electrons return to low-energy states and the spin moment is restored. It is clear that within RBA, the spin moment reduction is much smaller than the experimental observation, but the reason is simple. Any transitions among band states [36] must obey the dipole selection rule; and any strong transitions

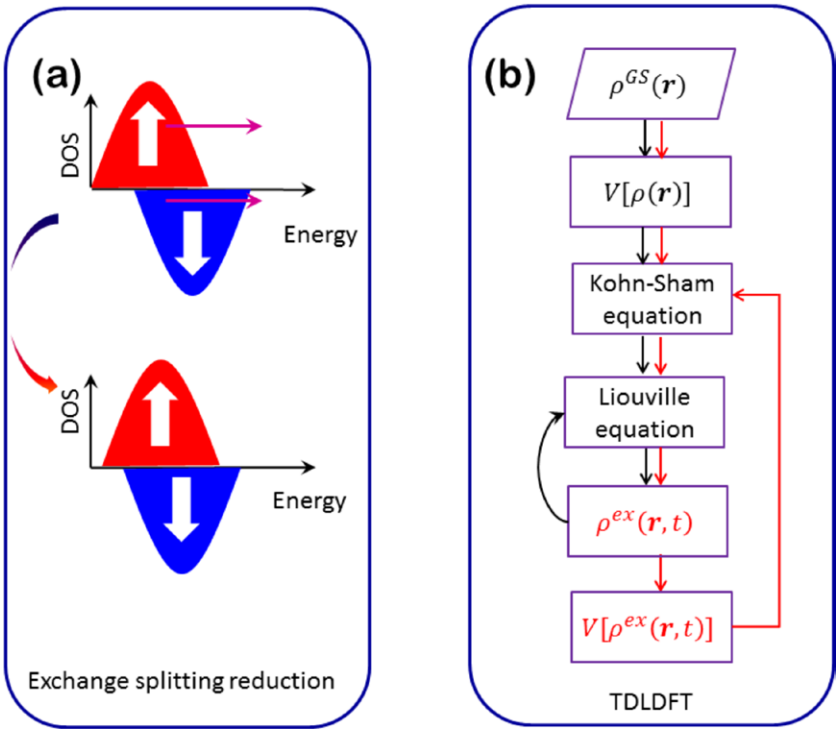

Figure 1. (a) Ultrafast laser-induced exchange splitting reduction. The laser pulse excites electrons out of the Fermi sea and weakens the exchange correlation. The minority and majority bands start to shift toward the Fermi level. (b) Flowchart of the time-dependent Liouville density functional theory (TDLDFT). The black arrows refer to the rigid-band approximation, while the red denote our new TDLDFT.

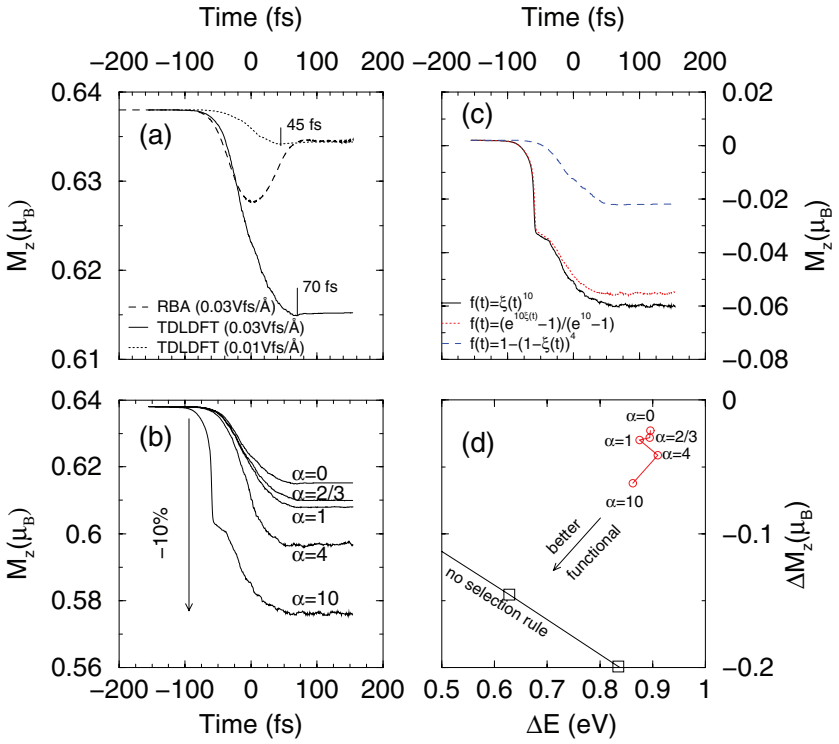

Figure 2. (a) Comparison of the spin moment reduction between the rigid-band approximation (dashed line, RBA) and the TDLDFT calculation (solid line, TDLDFT) as a function of time. The dotted line denotes the spin change when the laser vector potential is reduced to $A_0 = 0.01$ V fs Å^{-1}. (b) Spin moment change as a function of the spin attenuation factor α. With the largest α, we achieve a 10% reduction. (c) Influence of the functionals on the spin change. The dotted line refers to the exponential functional, while the long-dashed one the power functional. (d) Spin moment change versus the absorbed energy. We expect that a better agreement with the experiment will be reached if we find a better excited (laser) functional. The empty boxes denote the prior results [51], without taking into account the selection rule.

must have a large transition matrix element, and their transition energy should match or be close to the photon energy of the incident light. However, in solids, only a small number of **k** points satisfy these conditions [36], which imposes a severe constraint on any theory. The superdiffusion model [18] has a larger spin moment reduction since the above conditions are abandoned, as verified in an earlier study [51]. In summary, RBA is a single-shot non-self-consistent calculation and misses the dynamic many-body effect on the system itself. Therefore, RBA fails to induce a strong demagnetization.

The situation is quite different for TDLDFT. The solid line in figure 2(a) shows that the spin moment computed with TDLDFT is reduced to 0.6149 μ_B, or 3.5%, nearly an order of magnitude larger than the RBA calculation. Note that both RBA and TDLDFT use the same laser parameters. Such a reduction is robust, regardless of the generalized gradient approximation (GGA) or local density approximation (LDA) used for the functional. Different from the RBA results, the spin moment minimum is no longer at 0 fs, but instead shifts to $\tau_M = 70$ fs; and the spin does not recover within 100 fs either, fully consistent with the experimental observation [1]. This is encouraging. We wonder whether TDLDFT can explain how the laser amplitude affects τ_M.

Experimentally it is well known [6, 60, 61] that τ_M becomes shorter with a weak laser, but theoretically, τ_M is nearly independent of the laser field amplitude within the rigid-band approximation, a finding that is often used as evidence for phonon involvement [6], which further complicates the issue. We consider two laser amplitudes, 0.01 and 0.03 V fs Å^{-1}. Figure 2(a) (see the vertical bars) shows that as we decrease the field vector potential from 0.03 to 0.01 V fs Å^{-1}, while keeping the rest of parameters fixed, τ_M indeed reduces from 70 to 45 fs. There is no need to invoke the phonon contribution. The reason for this dependence is straightforward. For a weaker laser, only those transition states with the transition energy matching the photon energy are strongly excited; as a result, their response is impulsive and faster. When the laser becomes stronger, the low-lying states close to the Fermi surface start to contribute, so the demagnetization slows down.

3.2. Functional for the excited states

While our results are encouraging, quantitatively our spin moment reduction is still lower than the experimental data. Krieger *et al* [19] did observe a much larger reduction, but with a laser amplitude at least two orders of magnitude higher than the experimental one. We want to understand anything missing from our theory. As discussed above, within DFT, many-body effects are included through the exchange-correlation functional, but all the density functionals in use are highly geared toward the ground-state properties; and there is no well-established functional for excited states if it exists. GGA strongly favors a magnetic solution in the ground state; DFT gives too high Curie temperatures for all the transition metals [62]. A common practice to overcome this problem is to compute the effective exchange interaction which gives a much better Curie temperature.

Ortenzi *et al* [63] suggested a different approach to rescale the exchange and correlation potential for the spin part, while keeping the charge potential fixed. However, the Ortenzi formalism is completely static. To describe the laser-induced ultrafast demagnetization, we develop their method into a time-dependence functional, with the spin-polarized potential

$$V_{\uparrow}^{\text{new}}(\mathbf{r},t) = \frac{1}{2}((1+f(t))\,V_{\uparrow}(\mathbf{r},t) + (1-f(t))\,V_{\downarrow}(\mathbf{r},t)), \quad (7)$$

$$V_{\downarrow}^{\text{new}}(\mathbf{r},t) = \frac{1}{2}((1+f(t))\,V_{\downarrow}(\mathbf{r},t) + (1-f(t))\,V_{\uparrow}(\mathbf{r},t)), \quad (8)$$

where $V_{\uparrow(\downarrow)}$ is the potential for spin up (down). $f(t)$ is the time-dependent spin scaling and is a functional of the spin density scaling factor ξ for the Stoner kernel. ξ is fit to the magnetic moment change with pressure ($\xi = 0.88$ in their case) [63]. Here we make two extensions. First, we choose $f(t) = \xi^{\alpha}$ (other forms are presented below); Ortenzi's functional is recovered if $\alpha = 1$. Second, we redefine ξ as the ratio of the spin moment to the initial value or $\xi(t) = M_z(t)/M_z(-\infty)$, so the time-dependent exchange-correlation potential is self-consistently rescaled by the spin moment change. Thus, in our formalism ξ is no longer a fitting parameter. Instead, it has a physical meaning as it attenuates the strength of the exchange-correlation potential to reflect the diffusive nature of the excited states [52] and builds in a memory effect [56]. This second step allows us to smoothly connect the ground-state functional, where $\xi(t) = 1$, to the excited-state functional, while keeping intact all the good features of density functionals in GGA or LDA.

Our algorithm gets the best of both worlds: from the density functional theory, we effectively avoid the many-body problem and on the excited potential get excited-state properties, while from Liouville dynamic formalism, we add 'time' to the original static DFT. This avoids the limitation of the tiny time step in TDDFT [56], unphysical absorption peak shifting [64], and the time-dependent response frequencies of the Kohn–Sham response function even in the absence of an external field [65]. It can be easily incorporated into all the existing codes. In our study, we have implemented this algorithm in the Wien2k code [55]. α is used to control the level of attenuation on the spin, which will be called the spin attenuation factor below. The first line in figure 2(b) is our data with $\alpha = 0$ (same as the solid line in figure 2(a)). We gradually enhance the spin attenuation factor α, *while keeping the rest of the parameters unchanged*, and we find that the amount of spin reduction increases sharply. The main shape of the spin moment reduction does not change much from $\alpha = 0$ to 4. When we increase α to 10, we find that the spin reduction reaches -10%, much closer to the experimental results [1]. This demonstrates the great potential of the density functional theory as an enabling theory to describe the strong demagnetization. Interestingly, at $\alpha = 10$, $M_z(t)$ shows a kink around -55 fs, before the final minimum is reached.

To better understand the demagnetization, we test two additional functionals,

$$f_1(t) = \frac{e^{10\xi(t)} - 1}{e^{10} - 1}, \tag{9}$$

$$f_2(t) = 1 - (1 - \xi(t))^4, \tag{10}$$

where $f_1(t)$ has an exponential dependence and $f_2(t)$ has a power dependence. Figure 2(c) shows the net reduction of the spin moment. The kink on $M_z(t)$ is directly connected to the highly nonlinear dependence of the functional on $\xi(t)$, thus appearing in both functionals. The power functional $f_2(t)$ has no such kink, since its nonlinearity is smaller than the other two. This points to a promising new frontier by developing new functionals for the laser excitation, or laser functional. To quantify how far we are away from the best functional, figure 2(d) shows the spin moment reduction versus the absorbed energy (the total energy difference $\Delta E = E_{\text{final}} - E_{\text{initial}}$) for each α. This is the absolute measure on the absolute energy and spin moment scale. Our target is the demagnetization line obtained by our prior study [51] without considering the optical selection rule (see the line with the empty boxes in the lower left corner in figure 2(d)), which agrees with the experimental result if we assume 12.5% absorption efficiency [51]. Note that our present energy convergence criterion is much smaller than the energy change reported in the figure. When $\alpha = 0$, both ΔM_z and ΔE are small. When we increase α to 2/3 and 1, we see that the system absorbs less energy, not more energy, but with a larger spin reduction, a single most important finding. This demonstrates that our algorithm samples a much broader energy space, where the spin moment reduction does not need lots of energy. Naturally, this trend can not hold for any α and for any functional. When we increase α to 4, the usual trend is restored, i.e. the larger ΔE, the larger ΔM_z. We strongly believe that if a better functional is found, a better agreement can be reached. In particular, we see that when we increase α to 10, our result is closer to the experimental one.

3.3. Collapse of the exchange splitting

The realization of the strong demagnetization opens the door to understand the exchange splitting reduction. Figures 3(a) and (b) show the density of d states at -200 fs (in the absence of the laser) and 150 fs (after the laser excitation). The Fermi level is set at 0 eV. It is clear that both the majority and minority bands shift toward the Fermi level, but the majority shifts more, a similar finding reported for $4f$ Gd [38]. As a result, the exchange splitting is significantly reduced, in agreement with the prior experimental results [39].

But the photoemission can not directly assign the exchange splitting quenching to the demagnetization, since it probes only a small portion of the Brillouin zone [41]. This missing link is provided in figures 3(c)–(e). Figure 3(c) reproduces the spin moment change for $\alpha = 4$. The peak energies for the majority and minority bands, E_{majority} and E_{minority}, are shown in figures 3(d) and (e), respectively. It is very clear that the demagnetization follows E_{majority} and E_{minority} closely. This result represents the first theoretical confirmation of a long speculation as to how the demagnetization and exchange splitting are correlated in ferromagnetic Ni. Since different

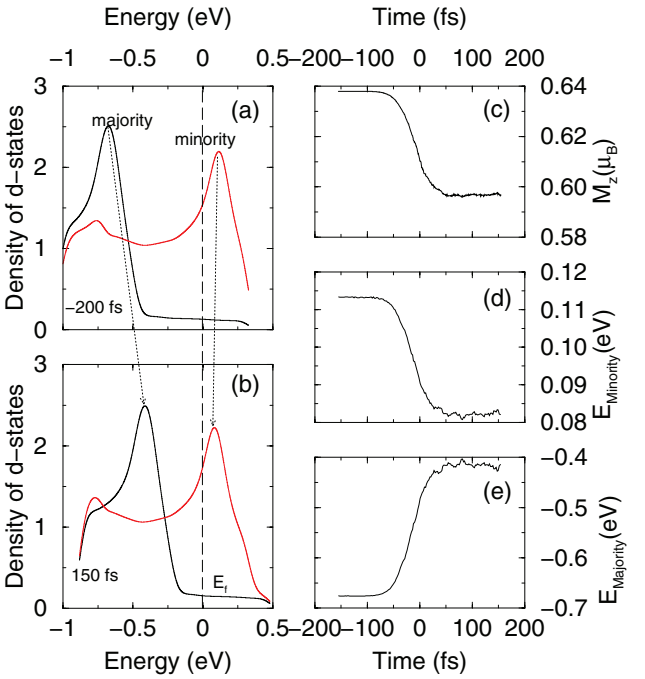

Figure 3. Density of $3d$ states (a) before and (b) after the laser excitation. The majority and minority peaks are clearly shifted toward the Fermi level, which is set at 0 eV. (c) Spin moment change as a function of time for a spin attenuation factor of $\alpha = 4$. (d) and (e) Peak energy of the minority and majority bands as a function of time. The majority band shifts 0.26 eV, while the minority 0.03 eV.

materials differ a lot in terms of the electronic and magnetic properties, further investigation is necessary for other materials. Recently, Andres *et al* [66] found the spin mixing in the surface state is not related to the exchange splitting change in Gd. Frietsch *et al* [67] suggested that the initial drop of the exchange splitting also follows the magnetic moment change in $5d$ electrons, not $4f$ electrons, but since their Landau–Lifshitz–Gilbert equation is module-conserved, they can only investigate the spin precession, not a true demagnetization. Our study provides a much needed theory.

3.4. Beyond density functional

The density functional theory represents a state-of-the-art first-principles technique to investigate the ground-state electronic and magnetic properties. To compute the excited states, DFT has intrinsic difficulties. First of all, nearly all the studies employ the ground-state functional to compute the excited-state properties. Second, in ferromagnets the spin wave excitation is formally not included in DFT, since only the density itself enters the theory. Our spin attenuation factor α only partially remedies this shortcoming. At $\alpha = 0$, the agreement with the experiment is poor, since the spin-polarized density is still not enough to weaken the exchange interaction. A larger α leads to a better agreement, since it reduces the exchange correlation more, but too big a value leads to an unphysical kink as seen in figure 2(b). A better functional is necessary.

To go beyond the density functional, one may include the relaxation of the collective spin waves excitation. However,

there are many-body interactions that are hard to treat. In the traditional spin wave theory, the spin moment reduction is due to the creation of magnons (spin wave quanta), often driven by a thermal field. The exchange splitting is certainly affected by the spin-wave relaxation. A weaker spin wave will lead to a smaller energy difference between the spin-up and spin-down electrons and a smaller spin moment overall. The difficulty is that the excitation by a femtosecond laser pulse is not the region that the spin wave theory can handle easily, since the interaction field is an electric field. One possible solution is to incorporate the spin wave excitation idea into the existing density functional theory, so the influence of the spin wave excitation on the exchange splitting and demagnetization can be closely examined. Clearly, additional research is needed along this direction.

4. Conclusion

We have developed an algorithm that integrates the time-dependent Liouville scheme into the density functional theory. Our algorithm respects the optical dipole selection rule. Importantly, this scheme overcomes two major hurdles—rigid-band approximation and ground-state density functional—and leads to a strong demagnetization. The key to our success is that we allow for the excited exchange-correlation potential to act upon the system itself, so those **k** points which are not optically accessible also experience the change of the excited-state potential. We show that without introducing an additional functional, a straightforward TDLDFT calculation leads to a 3.5% reduction, nearly an order of magnitude higher than the rigid-band approximation results. Once we introduce the Ortenzi functional, the maximum reduction within our current functionals reaches 10%. We expect that with a better functional, a better agreement with the experiment can be reached in the future. As a direct consequence of our current study, we can now directly correlate the exchange splitting quenching to the demagnetization, confirming the prior time- and spin-resolved photoemission experiments. Since our method is relatively simpler than TDDFT, we may be allowed to suggest that our method may find some applications to laser-induced ultrafast dynamics in high-temperature superconductors and other complex magnets. These systems have many more atoms in a unit cell, so the TDDFT calculation might be extremely time consuming. Another advantage that we notice is that it may include the lattice vibration at a lower cost. Research along this direction is underway.

Acknowledgments

This work was solely supported by the U.S. Department of Energy under Contract No. DE-FG02-06ER46304. Part of the work was done on Indiana State University's quantum cluster and high-performance computers. The research used resources of the National Energy Research Scientific Computing Center, which is supported by the Office of Science of the U.S. Department of Energy under Contract No. DE-AC02-05CH11231. This work was performed, in part, at the Center for Integrated Nanotechnologies, an Office of Science User Facility operated for the U.S. Department of Energy (DOE) Office of Science by Los Alamos National Laboratory (Contract DE-AC52-06NA25396) and Sandia National Laboratories (Contract DE-AC04-94AL85000).

References

[1] Beaurepaire E, Merle J C, Daunois A and Bigot J-Y 1996 *Phys. Rev. Lett.* **76** 4250
[2] Zhang G P, Hübner W, Beaurepaire E and Bigot J-Y 2002 *Top. Appl. Phys.* **83** 245
[3] Kirilyuk A, Kimel A V and Rasing Th 2010 *Rev. Mod. Phys.* **82** 2731
[4] Stanciu C D, Hansteen F, Kimel A V, Kirilyuk A, Tsukamoto A, Itoh A and Rasing Th 2007 *Phys. Rev. Lett.* **99** 047601
[5] Zhang G P and Hübner W 2000 *Phys. Rev. Lett.* **85** 3025
[6] Koopmans B, Malinowski G, Dalla Longa F, Steiauf D, Fähnle M, Roth T, Cinchetti M and Aeschlimann M 2010 *Nat. Mater.* **9** 259
[7] Lefkidis G and Hübner W 2009 *J. Magn. Magn. Mater.* **321** 979
[8] Carva K, Battiato M, Legut D and Oppeneer P M 2013 *Phys. Rev.* B **87** 184425
[9] Krauß M, Roth T, Alebrand S, Steil D, Cinchetti M, Aeschlimann M and Schneider H 2009 *Phys. Rev.* B **80** 180407
[10] Zhang G P, Bai Y, Hübner W, Lefkidis G and George T F 2008 *J. Appl. Phys.* **103** 07B113
[11] Zhang G P, Bai Y and George T F 2009 *Phys. Rev.* B **80** 214415
[12] Lefkidis G, Zhang G P and Hübner W 2009 *Phys. Rev. Lett.* **103** 217401
[13] Chaudhuri D, Xiang H P, Lefkidis G and Hübner W 2014 *Phys. Rev.* B **90** 245113
[14] Töws W and Pastor G M 2015 *Phys. Rev. Lett.* **115** 217204
[15] Essert S and Schneider H C 2011 *Phys. Rev.* B **84** 224405
[16] Illg C, Haag M and Fähnle M 2013 *Phys. Rev.* B **88** 214404
[17] Baral A, Vollmar S and Schneider H C 2014 *Phys. Rev.* B **90** 014427
[18] Battiato M, Carva K and Oppeneer P M 2012 *Phys. Rev.* B **86** 024404
[19] Krieger K, Dewhurst J K, Elliott P, Sharma S and Gross E K U 2015 *J. Chem. Theory Comput.* **11** 4870
[20] Schellekens A J and Koopmans B 2013 *Phys. Rev. Lett.* **110** 217204
[21] Guidoni L, Beaurepaire E and Bigot J-Y 2002 *Phys. Rev. Lett.* **89** 017401
[22] Vahaplar K *et al* 2012 *Phys. Rev.* B **85** 104402
[23] Eschenlohr A *et al* 2013 *Nat. Mater.* **12** 332
[24] Rudolf D *et al* 2012 *Nat. Commun.* **3** 1037
[25] Schellekens A J, Verhoeven W, Vader T N and Koopmans B 2013 *Appl. Phys. Lett.* **102** 252408
[26] Wietstruk M *et al* 2011 *Phys. Rev. Lett.* **106** 127401
[27] Sandratskii L M and Mavropoulos P 2011 *Phys. Rev.* B **83** 174408
[28] Mathias S *et al* 2012 *Proc. Natl Acad. Sci.* **109** 4792
[29] Mangin S *et al* 2014 *Nat. Mater.* **13** 286
[30] Moisan N *et al* 2014 *Sci. Rep.* **4** 4658
[31] Turgut E *et al* 2013 *Phys. Rev. Lett.* **110** 197201
[32] Koopmans B, van Kampen M, Kohlhepp J T and de Jonge W J M 2000 *Phys. Rev. Lett.* **85** 844
[33] Zhang G P, Hübner W, Lefkidis G, Bai Y and George T F 2009 *Nat. Phys.* **5** 499
[34] Zhang G P 2012 *Phys. Rev.* B **85** 224407

[35] Zhang G P, Bai Y H and George T F 2015 *Europhys. Lett.* **112** 27001
[36] Si M S, Li J Y, Yang D Z, Xue D S and Zhang G P 2014 *Sci. Rep.* **4** 5010
[37] Scholl A *et al* 1997 *Phys. Rev. Lett.* **79** 5146
[38] Carley R *et al* 2012 *Phys. Rev. Lett.* **109** 0574012
[39] Rhie H-S, Dürr H A and Eberhardt W 2003 *Phys. Rev. Lett.* **90** 247201
[40] Pickel M, Schmidt A B, Giesen F, Braun J, Minar J, Ebert H, Donath M and Weinelt M 2008 *Phys. Rev. Lett.* **101** 066402
[41] Weber A, Pressacco F, Günther S, Mancini E, Oppeneer P M and Back C H *Phys. Rev.* B **84** 132412
[42] Carpene E, Hedayat H, Boschini F and Dallera C 2015 *Phys. Rev.* B **91** 174414
[43] Harrison W A 2004 *Elementary Electronic Structure* (Singapore: World Scientific)
[44] Kira M and Koch S W 2011 *Semiconductor Quantum Optics* (Cambridge: Cambridge University Press)
[45] Haug H and Koch S W 2009 *Quantum Theory of the Optical and Electronic Properties of Semiconductors* 5th edn (Singapore: World Scientific)
[46] Lee M S and Mahanti S D 2012 *Phys. Rev.* B **85** 165149
[47] Lindberg M and Koch S W 1988 *Phys. Rev.* B **38** 3342
[48] Lingos P C, Wang J and Perakis I E 2015 *Phys. Rev.* B **91** 195203
[49] Mueller B Y, Baral A, Vollmar S, Cinchetti M, Aeschlimann M, Schneider H C and Rethfeld B 2013 *Phys. Rev. Lett.* **111** 167204
[50] Wang Z, Li S-S and Wang L-W 2015 *Phys. Rev. Lett.* **114** 063004
[51] Zhang G P, Si M S, Bai Y H and George T F 2015 *J. Phys.: Condens. Matter* **27** 206003
[52] Zhang G P, Gu M Q and Wu X S 2014 *J. Phys.: Condens. Matter* **26** 376001
[53] Mentink J H and Eckstein M 2014 *Phys. Rev. Lett.* **113** 057201
[54] Li T, Patz A, Mouchliadis L, Yan J, Lograsso T A, Perakis I E and Wang J 2013 *Nature* **496** 69
[55] Blaha P, Schwarz K, Madsen G K H, Kvasnicka D and Luitz J 2001 *WIEN2k, An Augmented Plane Wave + Local Orbitals Program for Calculating Crystal Properties* ed K Schwarz (Austria: Techn. Universität Wien)
[56] Marques M A L, Ullrich C A, Nogueira F, Rubio A, Burke K and Gross E K U (ed) 2006 *Time-Dependent Density Functional Theory* (*Lecture Notes in Physics* vol 706) (Berlin: Springer)
[57] Zhang G P 2011 *J. Phys.: Condens. Matter* **23** 206005
[58] Zhang G P and Hübner W 1999 *J. Appl. Phys.* **85** 5657
[59] Ambrosch-Draxl C and Sofo J O 2006 *Comput. Phys. Commun.* **175** 1
[60] Carpene E, Mancini E, Dallera C, Puppin E and De Silvestri S 2010 *Thin Solid Films* **519** 1642
[61] La-O-Vorakiat C *et al* 2012 *Phys. Rev.* X **2** 011005
[62] Kübler J 2000 *Theory of Itinerant Electron Magnetism* (Oxford: Oxford Science Publications) p 336
[63] Ortenzi L, Mazin I I, Blaha P and Boeri L 2012 *Phys. Rev.* B **86** 064437
[64] Provorse M R, Habenicht B F and Isborn C M 2015 *J. Chem. Theory Comput.* **11** 4791
[65] Fuks J I, Luo K, Sandoval E D and Maitra N T 2015 *Phys. Rev. Lett.* **114** 183002
[66] Andres B, Christ M, Gahl C, Wietstruk M, Weinelt M and Kirschner J 2015 *Phys. Rev. Lett.* **115** 207404
[67] Frietsch B, Bowlan J, Carley R, Teichmann M, Wienholdt S, Hinzke D, Nowak U, Carva K, Oppeneer P M and Weinelt M 2015 *Nat. Commun.* **6** 8262